Electronic Supplementary Material (ESI) for CrystEngComm.

A 2-fold interpenetrated zinc-organic framework with triazole sites: luminescent sensing of Fe^{3+} and $Cr_2O_7^{2-}$, and warm white-light emission by Ln^{3+} ions encapsulated

Bowen Qin,[a, b] *Xiaoying Zhang,**, [a] *Jiangyan Dang,*[a] *Dan Yue,*[b] *Bing Zhang,*[b] *Weidong Li,*[b] *Godefroid Gahungu,*[c] *Zhenling Wang,**, [b] *and Jingping Zhang**, [a]

[a] Advanced Energy Materials Research Center, Faculty of Chemistry, Northeast Normal University, Changchun 130024, P. R. China

[b] College of Materials Engineering, Henan International Joint Laboratory of Rare Earth Composite Materials, Henan University of Engineering, Zhengzhou 451191, P. R. China

[c] Department of Chemistry, University of Burundi, BP 2700, Bujumbura, BURUNDI

Table S1. Crystallographic data for compound **1**.

Compound	Compound **1**
empirical formula	$C_{49}H_{55}N_9O_{17}Zn_2$
formula weight	1172.79
T [K]	293.15
crystal system	Triclinic
space group	P
a [Å]	14.498
b [Å]	14.504
c [Å]	17.761
α [°]	84.51
β [°]	79.25
γ [°]	61.42
V	3222.0
Z	2
ρ_{calcd} [g cm^{-3}]	0.909
μ [mm^{-1}]	0.785
F(000)	896
reflections collected	60593
independent reflections	12270
GOF	1.045
R_1,[a] $I > 2\sigma(I)$	0.0538
wR_2,[b] $I > 2\sigma(I)$	0.1681

Table S2. Selected bond distances (Å) and bond angles (°) for complex **1**.

Zn(1)-O(1)	1.974(3)	Zn(2)-O(5)#1	1.960(3)
Zn(1)-O(2)	2.396(3)	Zn(2)-O(7)	1.986(3)
Zn(1)-O(4)#1	1.978(3)	Zn(2)-O(9)#2	2.291(3)
Zn(1)-O(6)	1.960(3)	Zn(2)-O(10)#2	2.015(3)
Zn(1)-N(1)	2.056(3)	Zn(2)-N(6)#3	2.045(3)
O(1)-Zn(1)-N(1)	108.03(12)	O(5)#1-Zn(2)-O(7)	101.36(12)
O(1)-Zn(1)-O(2)	58.52(13)	O(5)#1-Zn(2)-O(10)#2	143.37(14)
O(1)-Zn(1)-O(4)#1	102.78(13)	O(5)#1-Zn(2)-N(6)#3	100.06(11)
O(4)#1-Zn(1)-N(1)	96.65(13)	O(5)#1-Zn(2)-O(9)#2	94.23(13)
O(4)#1-Zn(1)-O(2)	160.79(14)	O(7)-Zn(2)-O(9)#2	153.94(13)
O(6)-Zn(1)-O(1)	133.49(13)	O(7)-Zn(2)-O(10)#2	96.49(13)
O(6)-Zn(1)-O(2)	86.67(12)	O(7)-Zn(2)-N(6)#3	99.14(12)
O(6)-Zn(1)-O(4)#1	106.25(13)	O(10)#2-Zn(2)-O(9)#2	59.63(13)
O(6)-Zn(1)-N(1)	103.81(13)	O(10)#2-Zn(2)-N(6)#3	108.38(13)
N(1)-Zn(1)-O(2)	93.88(13)	N(6)#3-Zn(2)-O(9)#2	98.53(13)

Symmetry transformations used to generate equivalent atoms: #1: x-1, y+1, z; #2: x, y-1, z; #3: x, y, z-1.

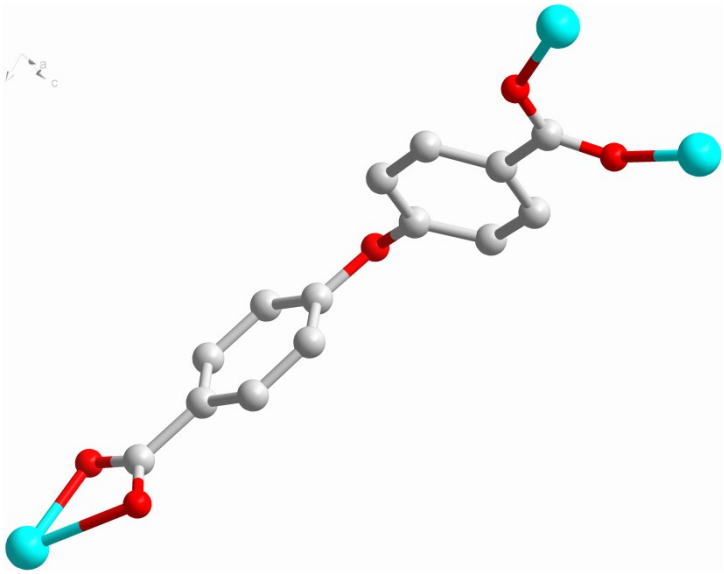

Fig. S1 The coordination mode of H_2OBA ligand.

Table S3. The comparison of Zn···Zn distance in paddle-wheel units with other reported works.

Compound name	Atom···Atom	Corresponding distance (Å)	References
HKUST-1	Cu···Cu	2.628	Science, 1999, 283, 1148-1150

$[\{Zn_2(abtc)(dmf)_2\}_3]\cdot 4H_2O\cdot 10dmf$	Zn···Zn	2.999	Angew. Chem., Int. Ed., 2008, 47, 7741-7745
MOF-508a	Zn···Zn	2.961	Angew. Chem. Int. Ed., 2006, 118, 1418-1421
MOF-508b	Zn···Zn	2.983	Angew. Chem. Int. Ed., 2006, 118, 1418-1421
$\{[Zn_2(BPnDC)_2(dabco)]\cdot 13DMF\cdot 3H_2O\}_n$	Zn···Zn	3.007	Chem. Eur. J., 2008, 14, 8812-8821
Zn-TCPP	Zn···Zn	2.948	Cryst. Growth Des., 2017, 17, 2090-2096
$Zn_2(\mu\text{-}OH)(dia)_2(sip)\cdot 2H_2O$	Zn···Zn	3.379	CrystEngComm, 2022, 24, 5450-5459
Compound **1**	Zn···Zn	3.458	This work

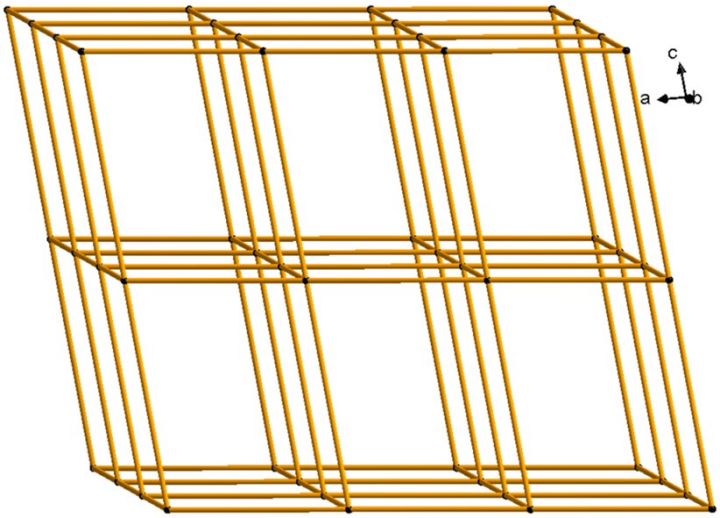

Fig. S2 Schematic illustration of the topologic framework of compound **1**.

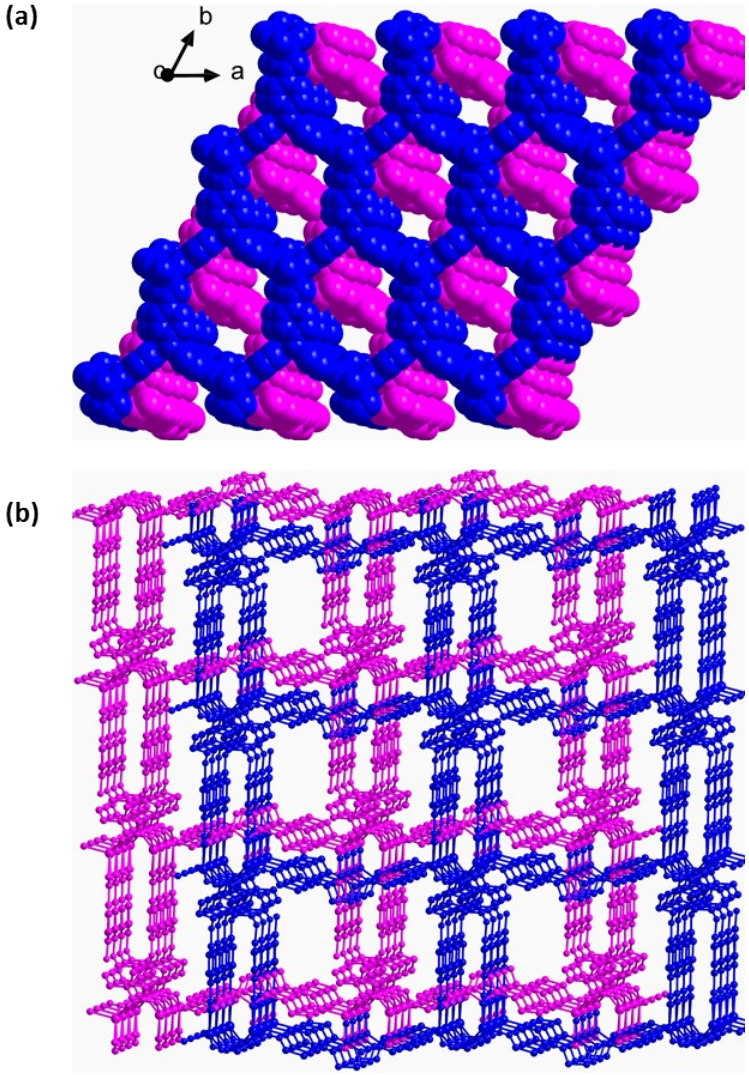

Fig. S3 Crystal structure of compound **1** with the 2-fold interpenetrated framework.

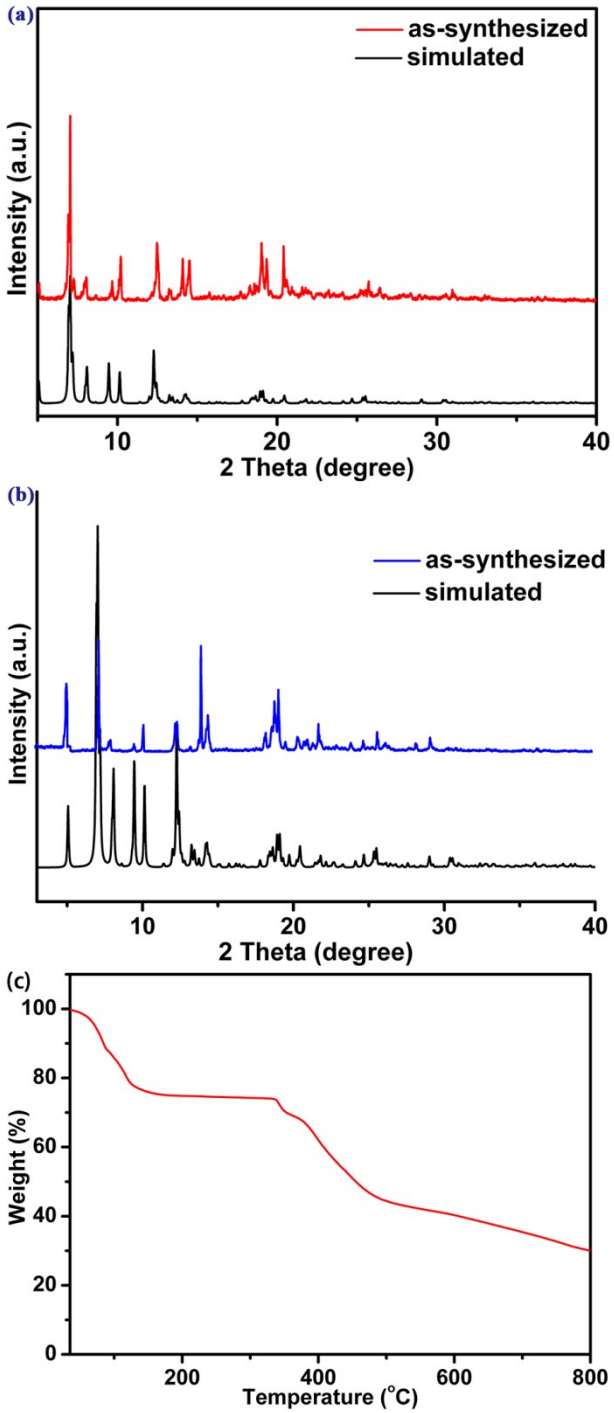

Fig. S4 (a) The PXRD spectra of complex **1** as prepared and simulated with the test angle of 5-40 degree; (b) The PXRD spectra of compound **1** as prepared and simulated with the test angle of 2-40 degree; (c) TGA curve of compound **1**. Thermogravimetric analysis curve of compound **1** shows 24% weight loss, which can be assigned to loss of 3 DMA and 4 H_2O molecules (cal. 24.84 %) from the crystal lattice.

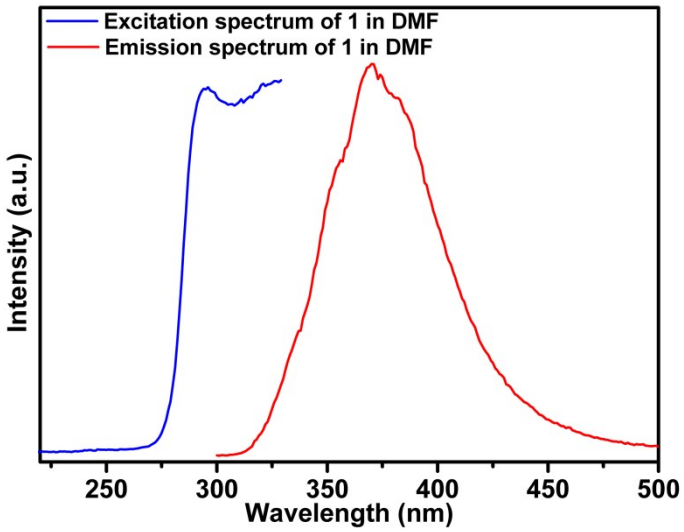

Fig. S5 The excitation spectrum and emission spectrum (excited on 290 nm) of compound **1** in DMF.

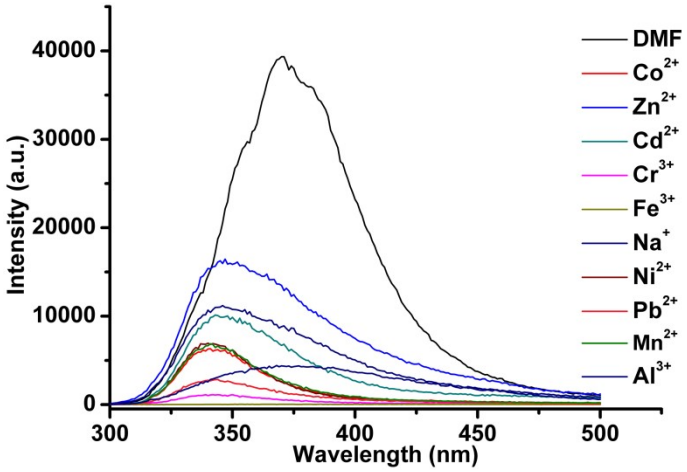

Fig. S6 Luminescence spectra of compound **1** (excited on 290 nm) in DMF with various nitrate salts (1 mM).

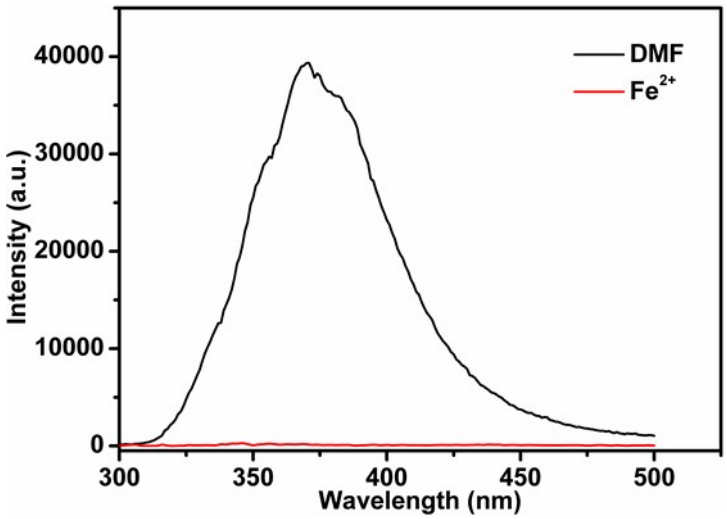

Fig. S7 Luminescence spectra of compound **1** (excited on 290 nm) before and after addition of Fe^{2+}.

Fig. S8 The photographs of compound **1** suspension treated with Fe^{3+} and $Cr_2O_7^{2-}$ taken under UV light excitation.

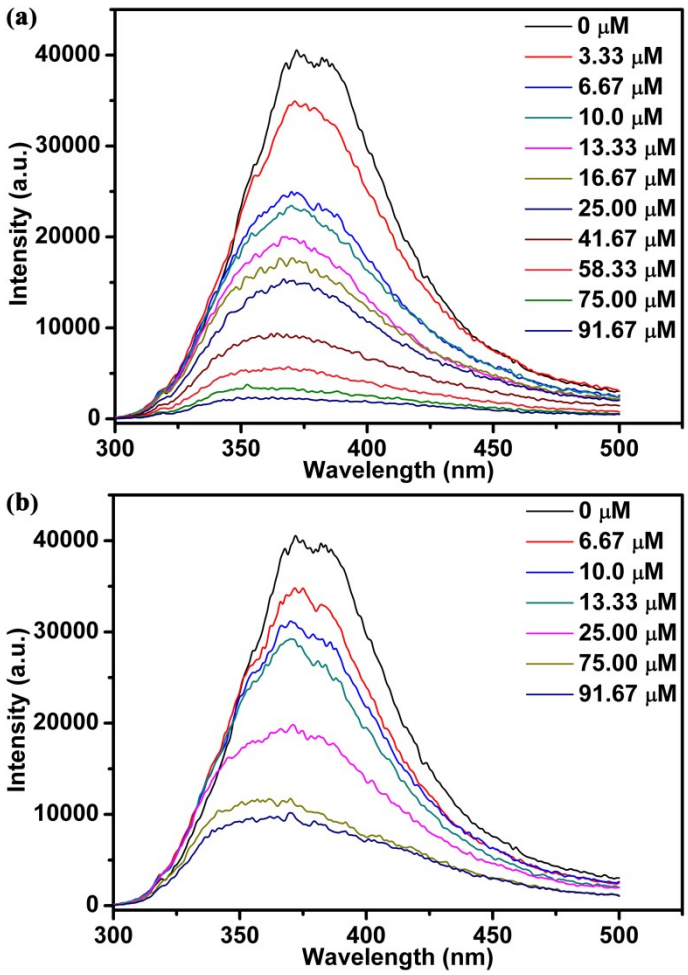

Fig. S9 Luminescence spectra (excited on 290 nm) of compound **1** suspension after treated with varying amounts of Fe^{3+} (a) and $Cr_2O_7^{2-}$ (b).

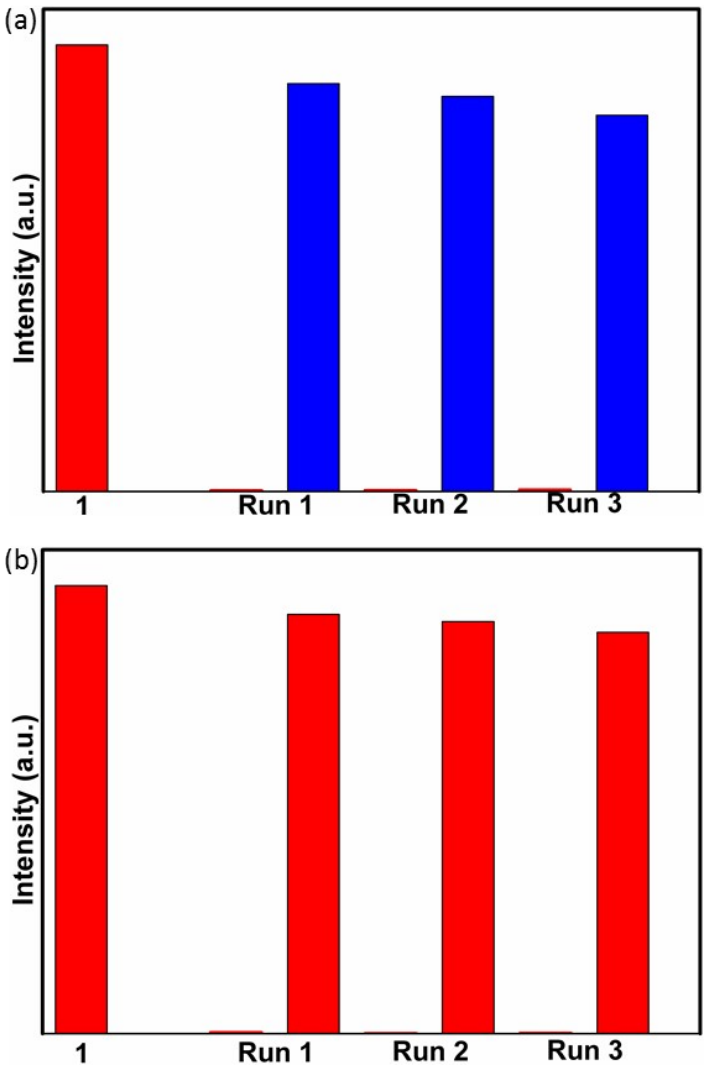

Fig. S10 Multiple cycles for the luminescent quenching of compound **1** by Fe^{3+}(a) and $Cr_2O_7^{2-}$(b) and recovery after washing by DMF for several times.

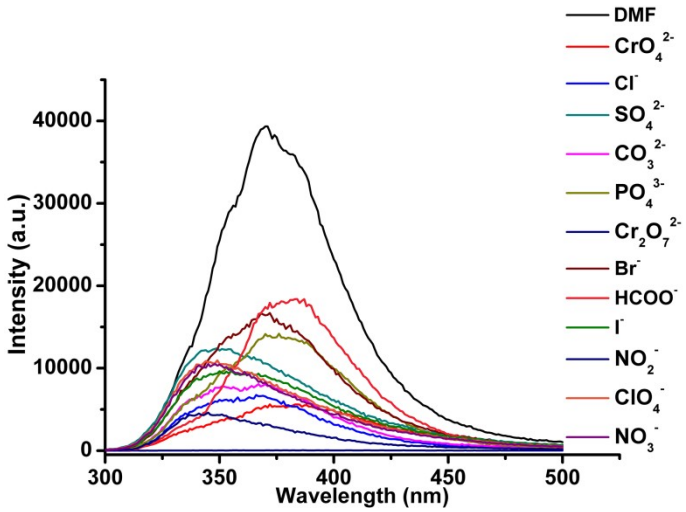

Fig. S11 Luminescence spectra (excited on 290 nm) of compound **1** suspension after treated with different anions.

Table S4. Comparison of K_{sv} and limits of detection among other reported materials and compound **1** as the Fe^{3+} sensor.

Compound name	K_{sv}, M^{-1}	Detection limit, μM	References
SLX-1		6.45	DaltonTrans., 2022, 51, 2890-2897
$\{[(CH_3)_2NH_2]_4[Ca_2Zn_4(L)_4]\cdot 4DMF\}_n$	4.36×10^3	18.8	CrystEngComm, 2020, 22, 4710-4715
Zn-MOF	3.93×10^4	0.90	Inorg. Chem., 2020, 59, 4588-4600
$[Zn(TIBTC)(DMA)]\cdot[NH_2(CH_3)_2]$	9.71×10^4	3.45	Inorg. Chem., 2020, 59, 8081-8098
$[Cd(TIBTC)(H_2O)]\cdot[NH_2(CH_3)_2]\cdot DMA$	2.43×10^4	5.51	
$[Zn_3(dpcp)_2(1,4'\text{-bmib})_2]_n$	40632	1.43	Cryst. Growth Des., 2021, 21, 5558-5572
$\{[Zn_4(dpcp)_2(4,4'\text{-bibp})_2(\mu_2\text{-}O)_4]\cdot 3H_2O\}_n$	143855	0.21	
$[Zn(2\text{-ata})(bidpe)]_n$	52732	0.57	
$[Zn(bbibp)(HCOO)_2]_n$	24713	1.36	
$[Bi(BTC)(H_2O)]\cdot H_2O$	2.02×10^4	1.59	Cryst. Growth Des., 2019, 19, 7217-7229
Eu-MOF	2.23×10^4	1.12	CrystEngComm, 2022, 24, 1358-1367
$[Co_2(4\text{-dptb})_2(1,3\text{-BDC})_2]\cdot 2H_2O$		5.84	Cryst. Growth Des., 2021, 21, 4390-4397
$[Zn(OBA)_2(L_1)\cdot 2DMA]_n$	4.22×10^4	1.06	Inorg. Chem., 2021, 60, 1716-1725
Compound **1**	7.69×10^4	0.58	This work
Eu^{3+}/Tb^{3+}@compound **1** (3:2)	4.606×10^4	0.98	This work

Table S5. Comparison of K_{sv} and limits of detection among other reported materials and compound **1** as the $Cr_2O_7^{2-}$ sensor.

Compound name	K_{sv}, M^{-1}	Detection limit, μM	References
$[Zn_2(tpeb)(bpdc)_2]$	1.08×10^4	1.07	Inorg. Chem., 2020, 59, 8818-8826
$[Zn_3(dpcp)_2(1,4'\text{-bmib})_2]_n$	5.32×10^4	0.71	Cryst. Growth Des., 2021, 21, 5558-5572
Eu-MOF	1.29×10^4	1.95	CrystEngComm, 2022, 24, 1358-1367
$[Co_2(4\text{-dptb})_2(1,3\text{-BDC})_2]\cdot 2H_2O$		6.51	Cryst. Growth Des., 2021, 21, 4390-4397

CSMCRI-5	1.73×10^4	none	Inorg. Chem., 2020, 59, 3012-3025
$[Bi(BTC)(H_2O)]\cdot H_2O$	1.95×10^4	1.64	Cryst. Growth Des., 2019, 19, 7217-7229
$\{[H_2N(Me)_2]_2[Zn_5(L)_2(OH)_2]\cdot 3DMF\cdot 4H_2O\}_n$	1.45×10^4	186	New J. Chem., 2022, 46, 4292-4299
$\{[Cd(L)(H_2O)_2]\cdot 4H_2O\}_n$	3.58×10^4	8.2	CrystEngComm, 2019, 21, 5185-5194
$[Zn(OBA)_2(L_1)\cdot 2DMA]_n$	1.2×10^4	3.87	Inorg. Chem., 2021, 60, 1716-1725
Compound **1**	3.28×10^4	1.37	This work
Eu^{3+}/Tb^{3+}@compound **1** (3:2)	2.16×10^4	2.08	This work

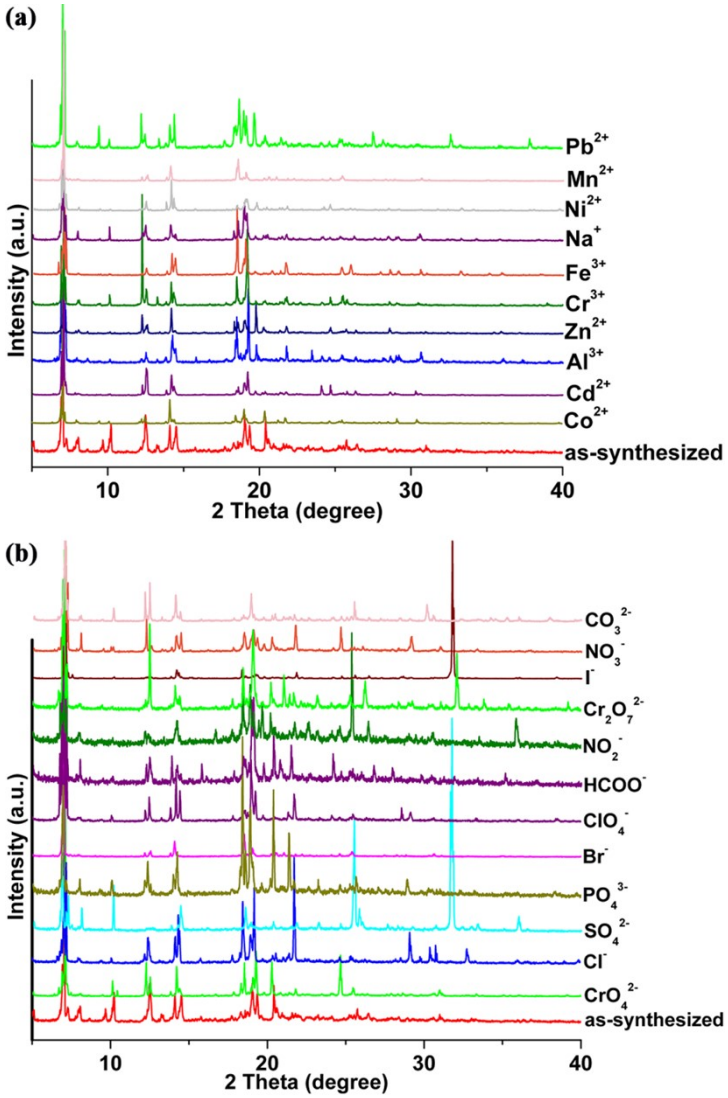

Fig. S12 The PXRD patterns of compound **1** after immersed in DMF solution containing cations (a) and anions (b) with concentration of 1 mM. Some ions enter the skeletons, making the diffraction peaks of this compound change partially.

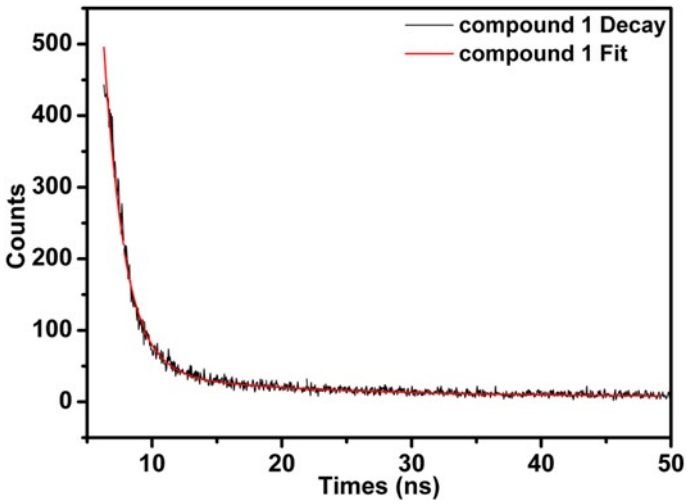

Fig. S13 The lifetime curves of compound **1**.

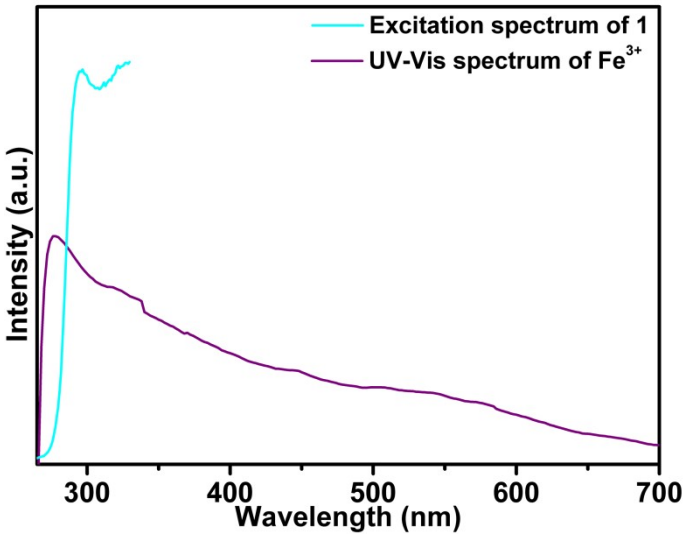

Fig. S14 The excitation spectrum of compound **1** and the UV-Vis adsorption spectra of Fe^{3+} in DMF.

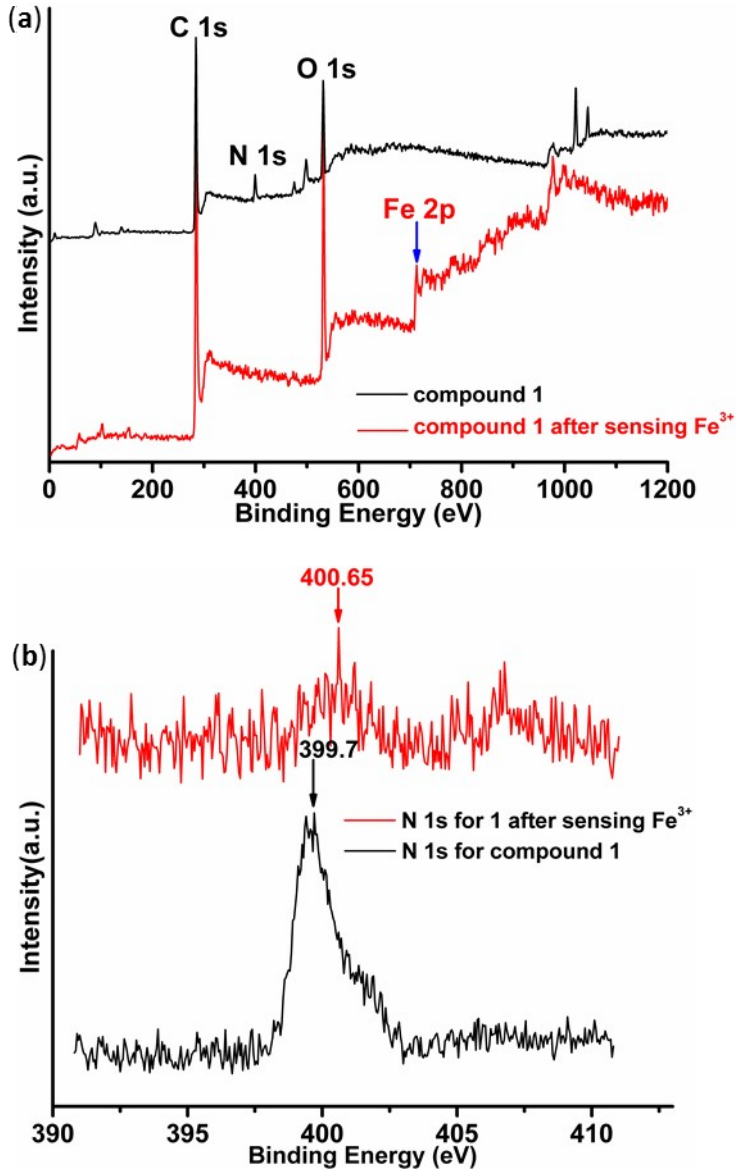

Fig. S15 (a) High-resolution XPS spectra of compound **1** before and after sensing Fe^{3+}; (b) High-resolution XPS spectra for the N 1s region of compound **1** before and after sensing Fe^{3+}.

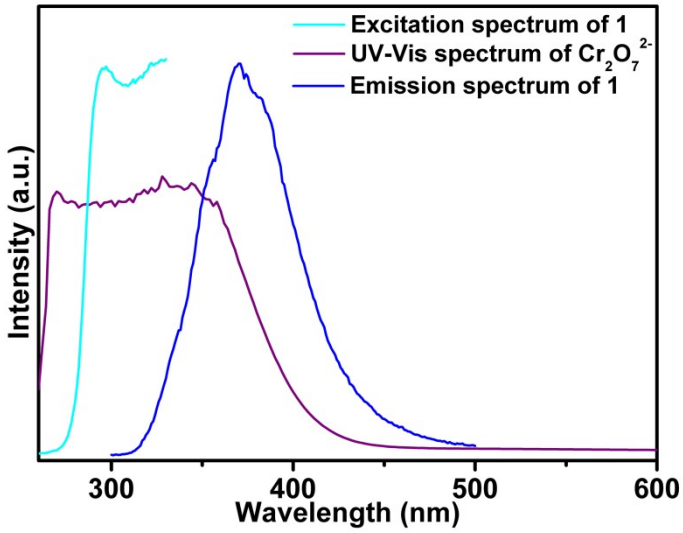

Fig. S16 The excitation and emission spectra of compound **1** and the UV-Vis adsorption spectra of $Cr_2O_7^{2-}$ in DMF.

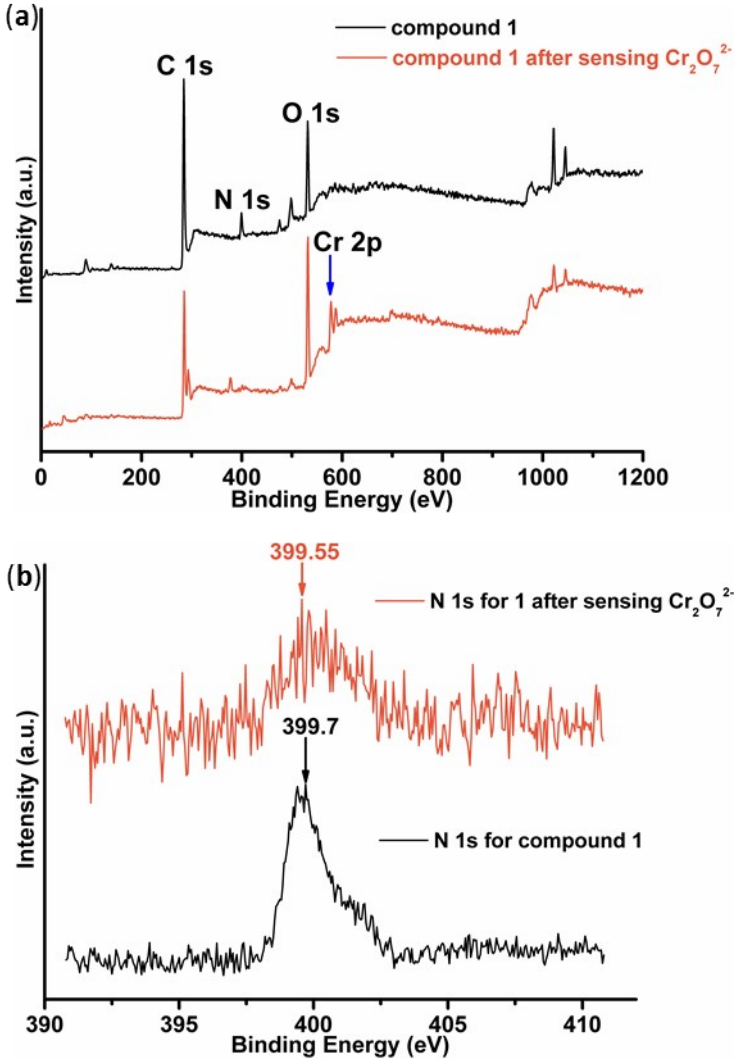

Fig. S17 (a) High-resolution XPS spectra of compound **1** before and after sensing $Cr_2O_7^{2-}$; (b) High-resolution XPS spectra for the N 1s region of compound **1** before

and after sensing $Cr_2O_7^{2-}$.

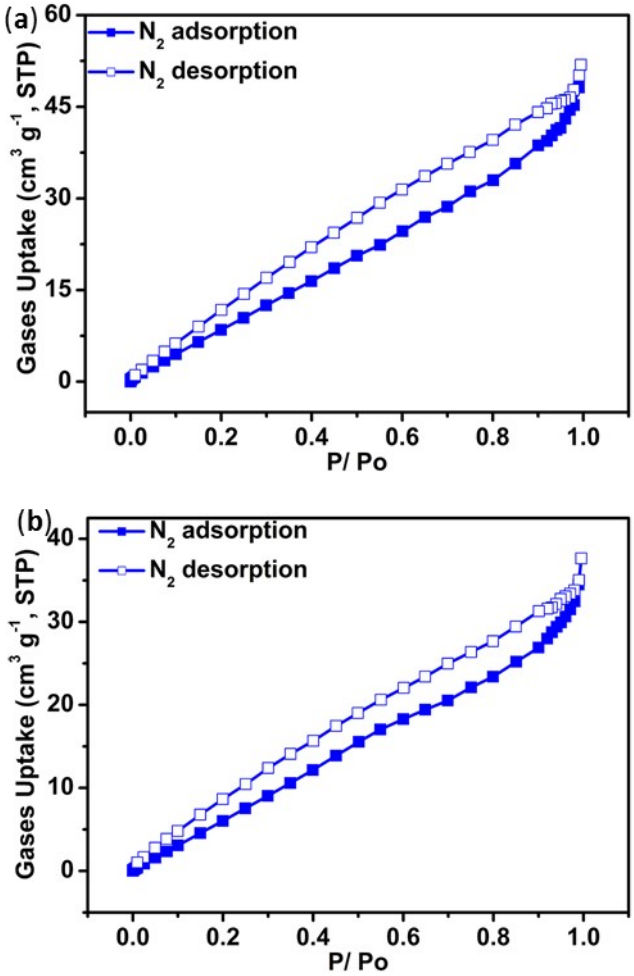

Fig. S18 The N_2 adsorption/desorption curve of compound **1** at 77 K with different exchange solvents (a: dichloromethane; b: methanol). The outgas temperature is 120°C. The gas desorption data with obvious hysteresis confirm a breathing behavior for compound **1**, suggesting the flexibility between the skeletons.

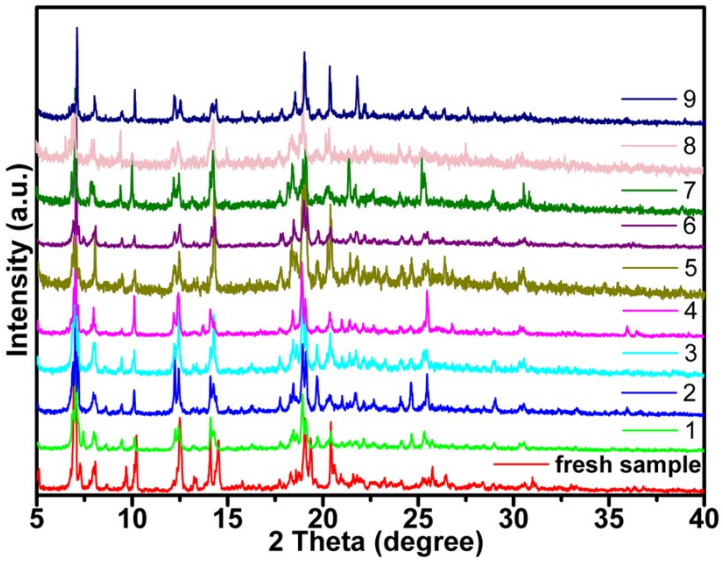

Fig. S19 The PXRD patterns of Ln^{3+}@compound **1**.

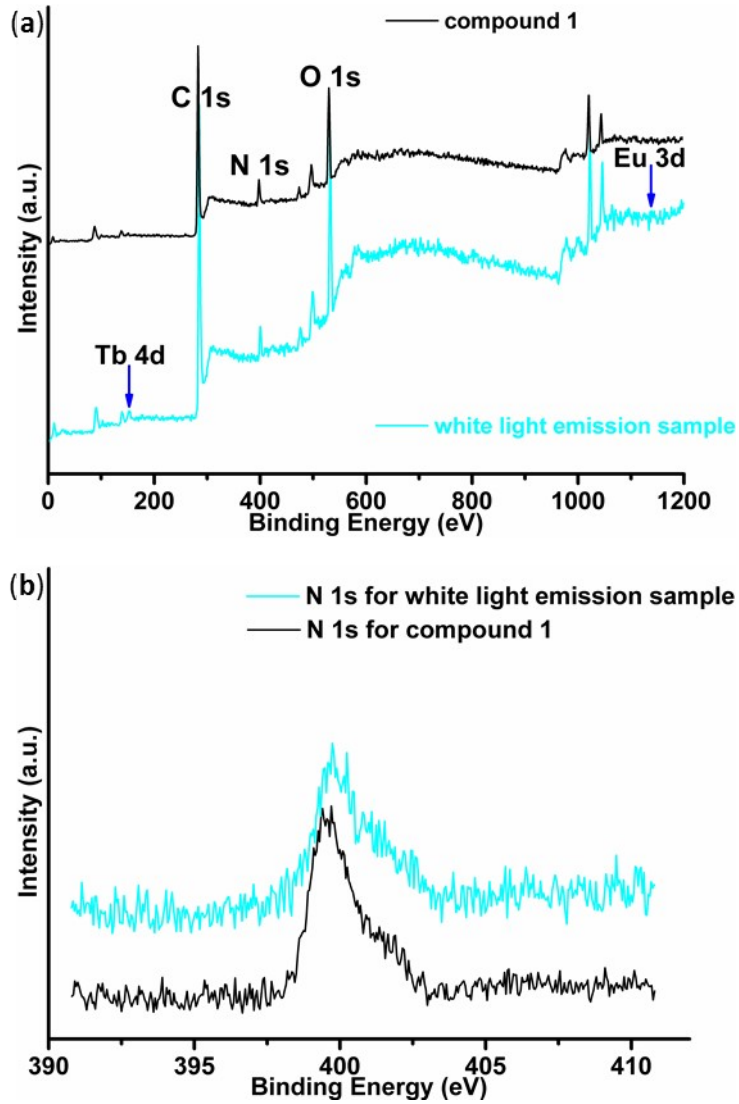

Fig. S20 (a) High-resolution XPS spectra of compound **1** before and after

encapsulating Ln^{3+}; (b) High-resolution XPS spectra for the N 1s region of compound **1** before and after encapsulating Ln^{3+}.

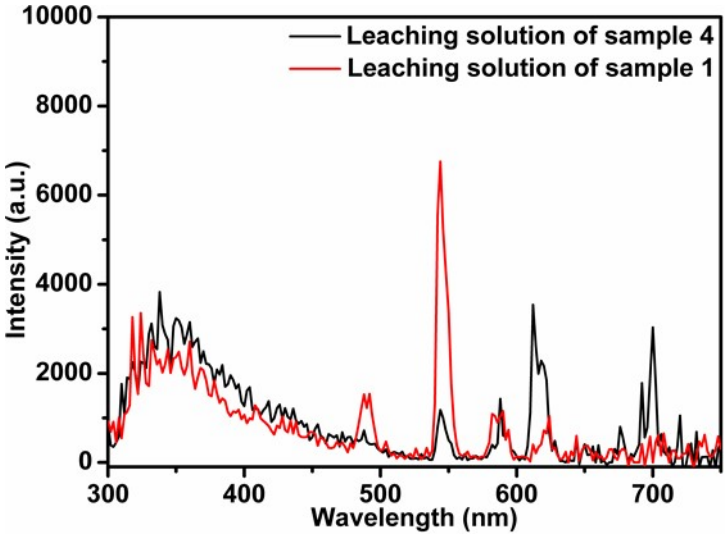

Fig. S21 The leaching tests of samples 1 and 4 performed in DMF.

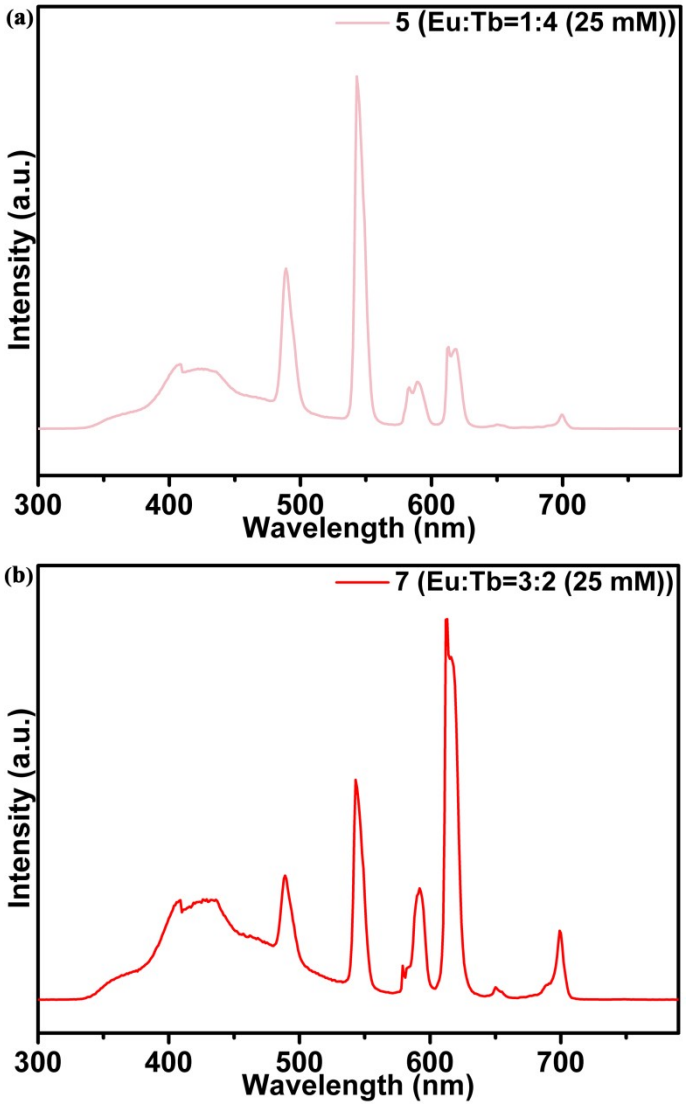

Fig. S22 The emission spectra of Eu/Tb-doped compound **1** (excited on 290 nm). The samples 5 and 7 were prepared by soaking 40 mg MOF in 10 mL DMF solutions containing 25 mM Ln^{3+} with different molar ration.

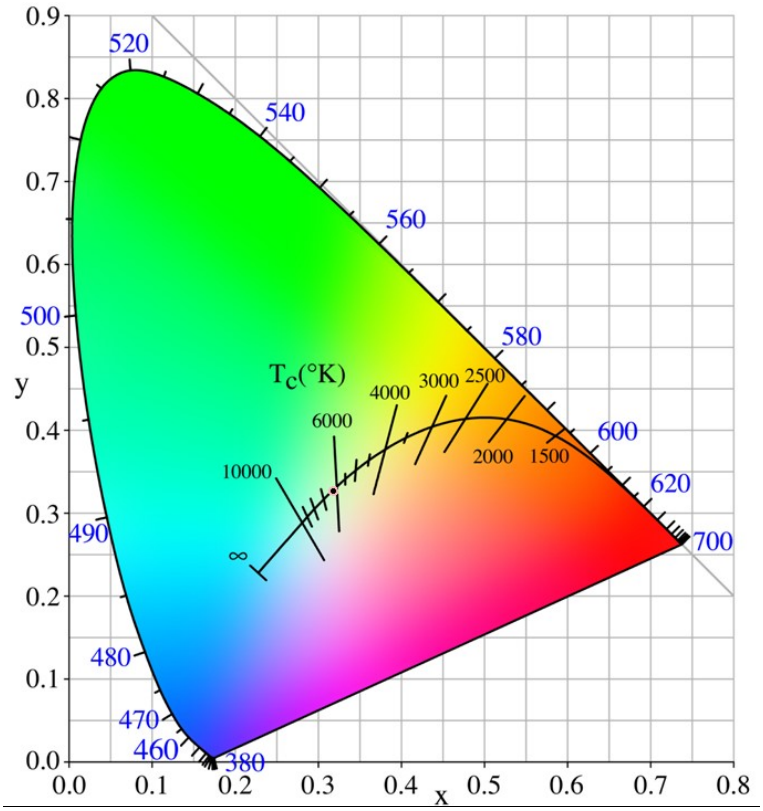

Fig. S23 The CIE chromaticity diagram of Eu^{3+}/Tb^{3+}@compound **1** with white-light emission.

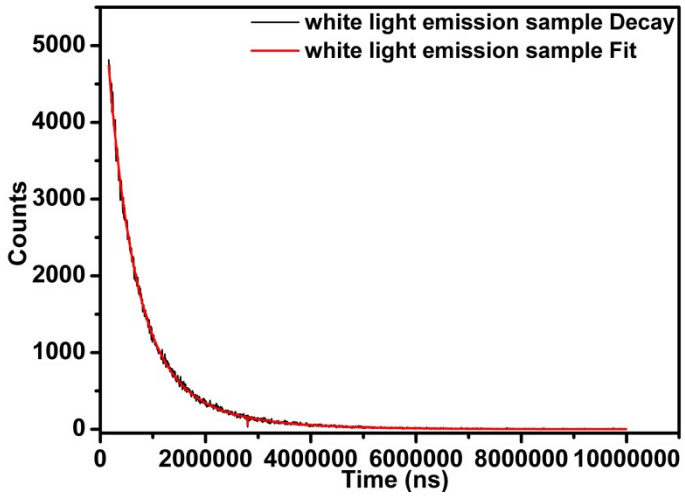

Fig. S24 The lifetime curves of white light emission sample.

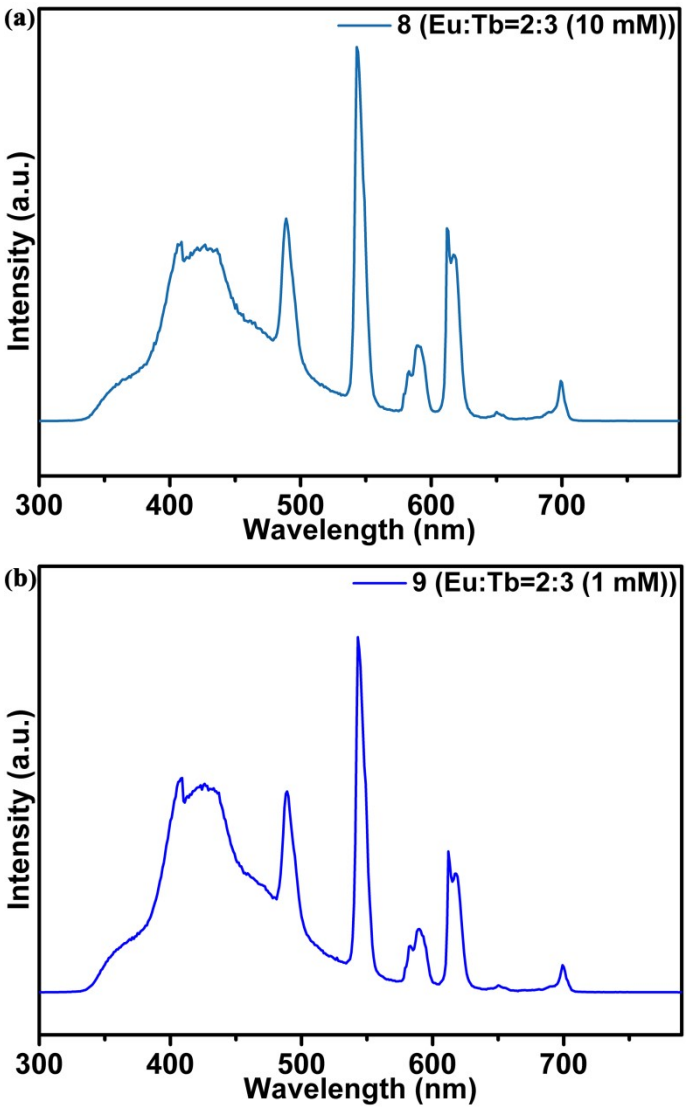

Fig. S25 The emission spectra of samples 8 and 9 prepared by soaking 40 mg compound **1** in 10 mL DMF solutions containing 10 mM (a) and 1 mM (b) Ln^{3+} with molar ration 2/3 (Eu/Tb) (excited on 290 nm).

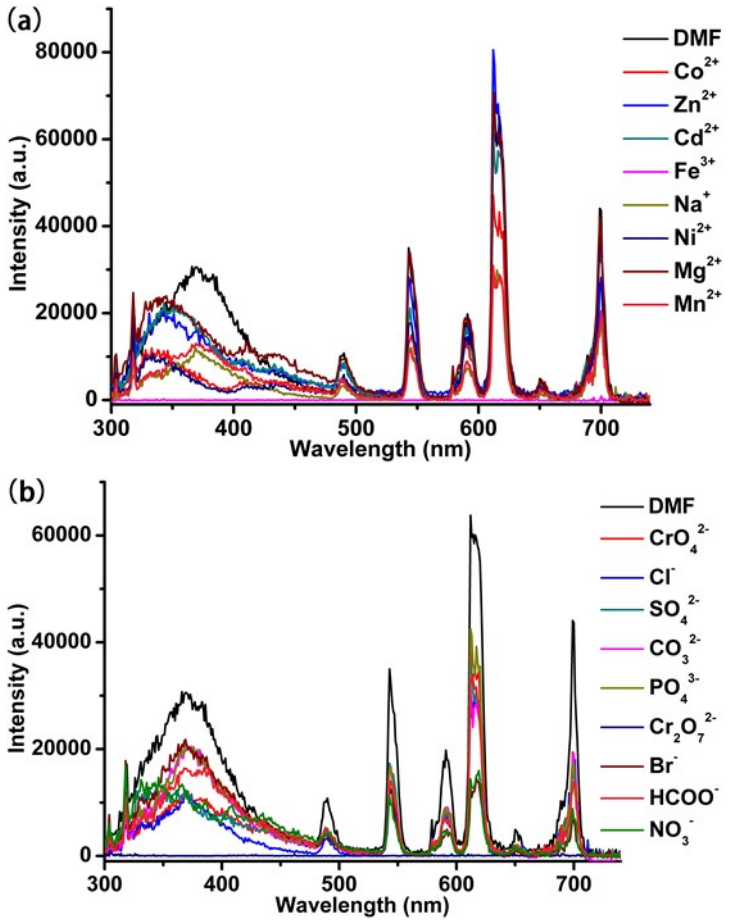

Fig. S26 Luminescent spectra of Eu^{3+}/Tb^{3+}@compound **1** (excited on 290 nm) in DMF with various cations (a) and anions (b) (1 mM), respectively.

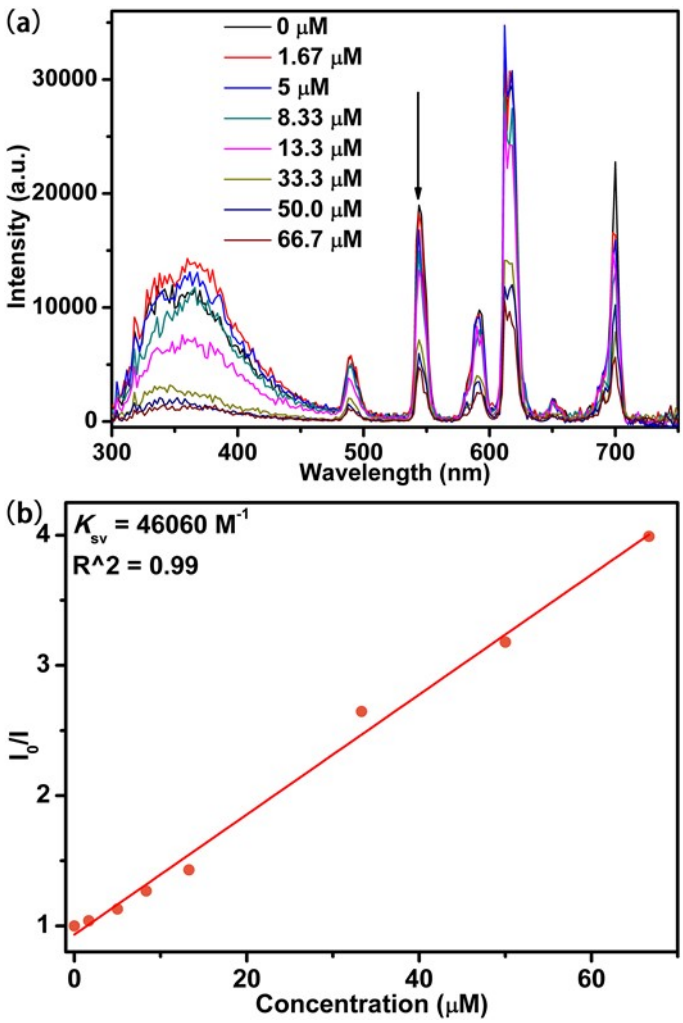

Fig. 27 The luminescent spectra (a) and Stern-Volmer plots (b) for sensing Fe^{3+} with different concentrations $Cr_2O_7^{2-}$ by compound **1**.

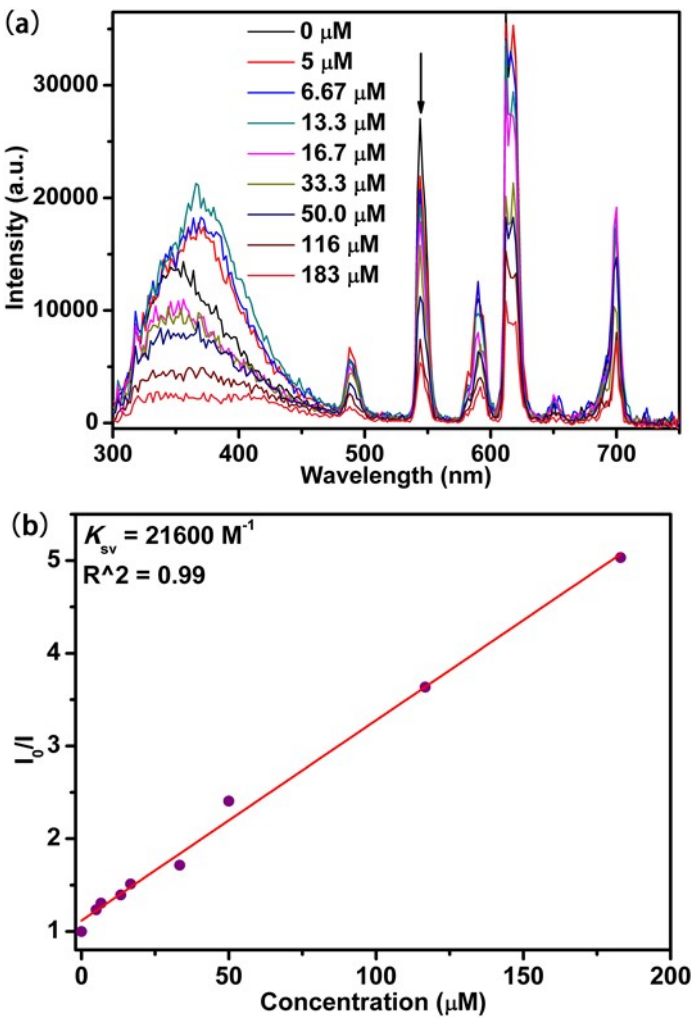

Fig. 28 The luminescent spectra (a) and Stern-Volmer plots (b) for sensing $Cr_2O_7^{2-}$ with different concentrations by compound **1**.